Fuel Processing Technology 206 (2020) 106466

Contents lists available at ScienceDirect

Fuel Processing Technology

journal homepage: www.elsevier.com/locate/fuproc

Research article

# Experimental studies on a two-step fast pyrolysis-catalytic hydrotreatment process for hydrocarbons from microalgae (*Nannochloropsis gaditana* and *Scenedesmus almeriensis*)

Neil Priharto[a,b], Frederik Ronsse[b], Wolter Prins[b], Robert Carleer[c], Hero Jan Heeres[d,*]

[a] School of Life Sciences and Technology, Institut Teknologi Bandung, Jalan Ganesha 10, Bandung 40132, Indonesia
[b] Department of Green Chemistry & Technology, Ghent University, Coupure links 653, 9000 Gent, Belgium
[c] Applied and Analytical Chemistry Research Group, Hasselt University, Agoralaan, Building D, 3590 Diepenbeek, Belgium
[d] Department of Chemical Engineering, ENTEG, University of Groningen, Nijenborgh 4, 9747 AG Groningen, the Netherlands

ARTICLE INFO

*Keywords:*
Microalgae
Fast pyrolysis
Catalytic hydrotreatment
Deoxygenation
Hydrotreated oils

ABSTRACT

Two microalgae species (marine *Nannochloropsis gaditana*, and freshwater *Scenedesmus almeriensis*) were subjected to pyrolysis followed by a catalytic hydrotreatment of the liquid products with the objective to obtain liquid products enriched in hydrocarbons. Pre-dried microalgae were pyrolyzed in a mechanically stirred fluidized bed reactor (380 and 480 °C) with fractional condensation. The heavy phase pyrolysis oils were hydrotreated (350 °C and 15 MPa of $H_2$ pressure for 4 h) using a NiMo on alumina catalyst. The pyrolysis liquids after pyrolysis and those after catalytic hydrotreatment were analyzed in detail using GC–MS, GC × GC–MS, and 2D HSQC NMR. The liquid products are enriched in aromatics and aliphatic hydrocarbons and, as such have a considerably lower oxygen content (1.6–4.2% w/w) compared to the microalgae feeds (25–30% w/w). The overall carbon yield for the liquid products was between 15.6 and 19.1% w/w based on the initial carbon content of the algae feedstock.

## 1. Introduction

The use of unconventional biomass for thermochemical conversion processes is gaining more and more interest in the last decade. A well-known example is the use of microalgae as the feed. Higher photosynthetic efficiency compared to lignocellulosic biomass, high biomass yields, and the non-competitiveness with food production are advantages of the use of microalgae as biomass feed [1–3]. Microalgae contain considerable amounts of lipids (7–26% w/w), carbohydrates (9–40% w/w), and proteins (27–61% w/w) [4–6]. The exact amount depends on the microalgae species and the cultivation techniques applied during production. A major advantage of the use of microalgae for thermochemical conversions is the low amount of recalcitrant lignin and lignin-derived compounds [7].

Microalgae enriched in lipids have shown high potential for biodiesel synthesis. However, thermochemical conversions (e.g., hydrothermal liquefaction and fast-pyrolysis) of microalgae have certain advantages. It allows conversion of the whole microalgae biomass into added-value products instead of the lipid/fatty acid fraction only as in the case of biodiesel production. Thermochemical conversions of microalgae have been reported in the literature [8–12]. For pyrolysis, three different products are formed viz., a condensed vapor known as pyrolysis oil, char, and non-condensable gases (NCGs). The liquid yield is heavily dependent on the microalgae species used, the presence of a catalyst, heating rate, residence time, and reaction temperature [12–14]. Several reactor configurations have been developed, all with the incentive to heat up the microalgae feedstock rapidly to avoid excessive char formation.

An overview of fast-pyrolysis studies using microalgae as the feed is given in Table 1. Typical oil yields cover a wide range and are between 18 and 65%. The reaction is conveniently conducted at temperatures ranging from 350 to 550 °C. Lower temperatures lead to lower liquid yields in favor of char, whereas higher temperatures lead to a higher amount of non-condensable gases. For instance, pyrolysis of *Chlorella vulgaris* at three different temperature (450, 500, and 550 °C) gave mainly char (42% w/w yield water-free basis) at 450 °C, whereas the highest liquid yield was obtained at 550 °C (47.7% w/w water-free basis) [15]. Fast pyrolysis of *Chlorella protothecoides* and *Microcystis aeruginosa* at 500 °C gave pyrolysis oil yields of 18 and 24% w/w, respectively [12].

* Corresponding author.
*E-mail address:* h.j.heeres@rug.nl (H.J. Heeres).

https://doi.org/10.1016/j.fuproc.2020.106466
Received 10 February 2020; Received in revised form 2 May 2020; Accepted 4 May 2020
Available online 24 May 2020

**Table 1**
Literature overview for fast pyrolysis studies on microalgae.

| No | Microalgae | Reactor type | Reaction temperature (°C) | Pyrolysis oil yield (% w/w) | Liquid product HHV (MJ $kg^{-1}$) | N content (% w/w) | Reference |
|---|---|---|---|---|---|---|---|
| 1 | *Chlorella protothecoides* and *Microcystis aeruginosa* | Fluid-bed reactor | 500 | 18–24 | – | 9.74–9.83 | [12] |
| 2 | *Chlorella vulgaris* | Continuous feeding auger reactor | 450–550 | 47.7 | 27–32 | – | [16] |
| 3 | *Chlorella vulgaris* and *Dunaliella salina* | Fixed-bed reactor | 300–700 | 30.9–64.9 | 12–23 | 6.5–10.8 | [15] |
| 4 | *Botryococcus braunii* residue | A three-port glass microreactor | 359–520 | – | – | – | [17] |
| 5 | *Dunaliella tertiolecta* lipid extracted-residue | Wire mesh captive sample type reactor | 450–750 | 33–45 | 22.2–23.5 | 7.1–9.83 | [18] |
| 6 | *Nannochloropsis* sp. whole cell and fractions | Fixed-bed reactor | 350–600 | 46–55 | – | 6.84 (whole cell), 10.36 (protein fraction) | [19] |

Compared to lignocellulosic pyrolysis oils, microalgae-derived pyrolysis oils have a higher High Heating Value (HHV), with values between 31 and 36 MJ $kg^{-1}$ [5]. Microalgae species with higher carbohydrate or lipid fractions tend to give pyrolysis oils with higher HHV's and lower oxygen contents [6]. Metabolically controlled *Chlorella protothecoides* grown heterotrophically gave a 3.4 fold increase in the pyrolysis oil yield, and the product showed several advantages compared to the non-metabolically modified version, such as a higher HHV and lower oil viscosity [1].

The chemical composition of pyrolysis oil from microalgae is complex and shows a mix of compounds belonging to different organic groups. The composition is a function of the pyrolysis conditions and type of microalgae feed [6]. In general, the components are categorized into high and lower molecular weight species. Typical low molecular weight components are hydrocarbons (saturated and unsaturated), phenolics compounds, carboxylic acids, alcohols, aldehydes, ketones and organic nitrogen-containing compounds.

Direct utilization of pyrolysis liquids is limited due to their limited thermal stability, high oxygen content, high water content, high viscosity, and immiscibility with hydrocarbons [20,21]. Also, the high amounts of nitrogen, mainly in the form of organo-nitrogen compounds in microalgae pyrolysis oils (Table 1), is not a favorable feature as it will result in NOx emissions during combustion and issues with the hydrotreating catalysts when co-processed in existing crude oil refineries [5].

Several technologies have been used to improve the properties of pyrolysis liquids. A well-known example is a catalytic hydrotreatment [20–24]. It involves reaction of the pyrolysis liquids with hydrogen gas at elevated temperatures and pressures in the presence of a solid catalyst [25,26]. Catalytic hydrotreatments are typically performed at 10–20 MPa of hydrogen pressure and temperatures ranging from 250 to 400 °C. During the hydrotreatment, several reactions occur, and examples are hydrogenation, hydrogenolysis, hydrodeoxygenation, decarboxylation, decarbonylation, cracking/hydrocracking, and polymerization reactions [26]. Typical catalysts for the hydrotreatment of pyrolysis oils are supported metal catalysts (e.g., noble metals on various supports). Sulphided transition metal catalysts (e.g., NiMo and CoMo), typically used in conventional hydrodesulphurization units in oil refineries, have also been applied [27–29].

An overview of hydrotreatment studies on microalgae-derived pyrolysis oils is given in Table 2. Catalytic hydrotreatment of microalgae derived pyrolysis oils is usually conducted at a temperature ranging from 250 to 350 °C at $H_2$ pressures between 2 and 18 MPa [30]. Oil yields cover a large range and are between 41 and 93% w/w. A study on the catalytic hydrotreatment of pyrolysis oils derived from *Chlorella* sp. and *Nannochloropsis* sp. at 350 °C and 2 MPa of $H_2$ pressure over bimetallic Ni-Cu/$ZrO_2$ catalysts show an 82% reduction of the oxygen content [30]. Catalytic hydrotreatment of *Chlorella* sp. over a Ni-Co-Pd/$\gamma$-$Al_2O_3$ catalyst at 300 °C and 2 MPa of $H_2$ pressure resulted in an 80.4% reduction of the oxygen content and hydrotreated pyrolysis oils in 90% w/w yield were obtained [31]. The hydrotreated oils contain a high amount of low molecular weight compounds (e.g., aromatics and alkylphenolics), which have the potential to be used as drop-in chemicals in existing petroleum refineries [31].

This study deals with a two-step approach to obtain liquids enriched in low molecular weight compounds from two different microalgae species (*Nannochloropsis gaditana* and *Scenedesmus almeriensis*). It involves an initial fast pyrolysis step in a mechanically stirred fluidized bed reactor with staged condensation of the condensable vapors, followed by a catalytic hydrotreatment of the heavy phase pyrolysis liquid in a batch reactor with a NiMo catalyst on alumina. The overall aim was to produce high-quality hydrotreated oils (e.g., low in oxygenates, low amounts of nitrogen compounds, and high hydrocarbon content) from microalgae with a high carbon efficiency to be used as transportation fuel or as a co-feed in an oil refinery. *Nannochloropsis gaditana* and *Scenedesmus almeriensis* were selected as the microalgae feed based on their high growth rates and low cultivation requirements. The product

**Table 2**
Literature overview for the catalytic hydrotreatment of microalgae-derived pyrolysis oils.

| Microalgae | Feed | Catalyst | Reaction T (°C) | $H_2$ pressure (MPa) | Feedstock oxygen content (% w/w) | Product oil oxygen content (% w/w) | Oil yields (% w/w) | Reference |
|---|---|---|---|---|---|---|---|---|
| *Chlorella* sp. | Catalytic pyrolysis oils | Trimetalic Ni-Co-Pd/$\gamma$-$Al_2O_3$ | 300 | 2 | 10.6 | 2.1 | 89.6 | [31] |
| *Chlorella* and *Nannochloropsis* sp. | Catalytic pyrolysis | Bimetallic Ni-Cu/$ZrO_2$ | 350 | 2 | 7.2–5.8 | 1.3–1.6 | – | [30] |
| *Spirulina* sp. | Bio-crude from continuous hydrothermal liquefaction | NiMo | 250–350 | 4–8 | 6.9 | 6.2–0.0 | – | [21] |
| *Chlorella* sp. | Bio-crude from hydrothermal liquefaction | NiMo and CoMo | 350 and 405 | 18.5 | 11.1–16.2 | 1–5 | 41–93.1 | [4] |

oils were analyzed using a range of analytical techniques (GC × GC-FID, GPC, and HSQC-NMR) to determine the molecular composition of the oils and to gain insights into molecular transformations during the hydrotreatment step. Finally, overall mass- and carbon balances were determined and will be discussed to evaluate the potential of the two-step concept.

## 2. Materials and methods

### 2.1. Feedstock, fluid bed material and catalyst

The marine microalgae *Nannochloropsis gaditana* (CCAP-849/5) and the freshwater microalgae *Scenedesmus almeriensis* (CCAP 276/24) were provided by the Estación Experimental Las Palmerillas, University of Almería, Spain. In the following, *Nannochloropsis gaditana* is abbreviated as NG and *Scenedesmus almeriensis* as SA. The freeze-dried feedstocks consisted of agglomerated particles. Both were ground and sieved to homogenous particles with sizes ranging between 2 and 3 mm.

Silica sand (PTB-Compaktuna, Gent, Belgium) with a particle density of 2650 kg $m^{-3}$ and a mean diameter of 250 μm was used as the bed material in the mechanically stirred fluidized bed pyrolysis reactor.

NiMo on alumina support (KF 848) was obtained from EuroCat and used as the catalyst in the catalytic hydrotreatment studies. The catalyst was sulphided using dimethyl disulphide (DMDS, Sigma-Aldrich) before each hydrotreatment reaction. High purity hydrogen gas (> 99.99% mol/mol) for hydrotreatment studies was obtained from Hoekloos (The Netherlands).

### 2.2. Analytical techniques

#### 2.2.1. Elemental analyses, energy content, thermogravimetric analysis, and ash content

The elemental composition (CHNSO) of the pyrolysis chars, heavy phase pyrolysis oils, and hydrotreated-oils were determined using a FLASH 2000 organic elemental analyzer (Thermo Fisher Scientific, Waltham, USA) equipped with a thermal conductivity detector (TCD) with CHNS and oxygen configuration. High purity helium (Alphagaz 1) from Air Liquide was used as the carrier and reference gas. High purity oxygen (Alphagaz 1), also from Air Liquide was used as the combustion gas. 2,5-(Bis(5-tert-butyl-2-benzo-oxazol-2-yl) thiophene (BBOT) was used as standard. All analyses were carried out in duplicate, and the average value is reported.

The higher heating value (HHV) of the heavy phase pyrolysis oils and hydrotreated-oils was determined using an E2K combustion calorimeter (Digital Data Systems, Gauteng, South Africa) using ascorbic acid as standard.

Thermogravimetric analysis (TGA) of the feedstocks was performed using a TGA 7 from PerkinElmer. The samples were heated under a nitrogen atmosphere with a heating rate of 10 °C $min^{-1}$ from 20 °C to 900 °C.

Inductively coupled plasma optical emission spectrometry (ICP-OES) was performed using a method described earlier [32] to determine the amounts of inorganics in the dried microalga feed.

#### 2.2.2. Gas-phase product analyses

The composition of the non-condensable fast pyrolysis gases (NCG) was determined off-line using an Agilent 490 Micro GC from Agilent Technologies. The gas sample was collected using a 100-ml gas-tight syringe. The micro GC was equipped with two TCD detectors and two analytical columns. The first column (10 m, 0.53 mm internal diameter (ID), Molesieve 5A -with backflush) was set at 75 °C to determine $H_2$, $N_2$, $CH_4$, and CO. The second column (10 m, 0.53 mm ID, PoraPak-Q) was set to 70 °C and used for the determination of $CO_2$, $C_2H_4$, $C_2H_6$, $C_3H_6$, and $C_3H_8$. High purity argon and helium (Alphagaz 1 from Air Liquide) were used as the carrier gas.

The composition of the gases from the catalytic hydrotreatments

was determined off-line using a GC (Hewlett Packard 5890 Series II) equipped with a thermal conductivity detector (GC-TCD). A Poraplot Q $Al_2O_3/Na_2SO_4$ column and a molecular sieve (5 Å) column were used for analysis. The injector temperature and the detector temperature were pre-set at 150 °C and 90 °C. The oven temperature was kept at 40 °C for 2 min, then heated to 90 °C at a rate of 20 °C $min^{-1}$ and kept at this temperature for 2 min. A reference gas supplied by Westfalen Gassen Nederland B.B. (55.19% mol/mol $H_2$, 19.70% mol/mol $CH_4$, 3.00% mol/mol CO, 18.10% mol/mol $CO_2$, 0.51% mol/mol ethylene, 1.49% mol/mol ethane, 0.51% mol/mol propylene and 1.50% mol/mol propane) was used to identify and quantify the components in the gas phase.

*2.2.3. Analyses of heavy phase pyrolysis oils and hydrotreated oils*

*2.2.3.1. GC–MS analyses.* Before GC–MS analyses, the heavy phase pyrolysis oils and hydrotreated oils were diluted to 1% w/w solutions in tetrahydrofuran (THF). Di-n-butyl ether (DBE) was added used as an internal standard (1000 ppm). Approximately 1 µl of the sample was directly injected into the GC–MS (Hewlett Packard 5890 GC) coupled to a Quadruple Hewlett Packard 6890 MSD with a sol–gel capillary column (60 m, 0.25 mm ID, and a 0.25 µm film, temperature program: 5 min at 40 °C, 3 °C $min^{-1}$ to 250 °C hold time 10 min) [33]. Quantification of the peak areas was done by integration of the.

Semi-quantification of the concentrations of the individual components was performed by comparing the peak areas (based on integration of total ion current (TIC)) the with that of the total peak area, which is typically used to quantify components in bioliquids with hundreds of individual components [34–36] Identification of the individual components was performed by comparing the spectra with those in the MS library from the National Institute of Standards and Technology (NIST).

*2.2.3.2. Two-dimensional (GC × GC) gas chromatography analyses.* GC × GC analyses were performed on a GC × GC-FID from JEOL equipped with a cryogenic trap system and two separate columns, viz. a RTX-1701 capillary column (30 m × 0.25 mm internal diameter and 0.25 µm film thickness) connected by a Meltfit to a Rxi-5Sil MS column (120 cm × 0.15 mm ID and 0.15 µm film thickness).

GC × GC-FID analyses parameters were described in a previous study [37]. The identification of the main component groups (e.g., alkanes, aromatics, alkylphenolics) in the heavy phase fast pyrolysis oils and hydrotreated oils were made by comparing the spectra of representative model compounds for the component groups. Quantification was performed by using an average relative response factor (RRF) per component group with di-n-butyl ether (DBE) as the internal standard. The sample was diluted to a 5% v/v solution using GC-grade tetrahydrofuran (Sigma-Aldrich), and 1 g $l^{-1}$ of di-n-butyl ether (DBE) (Sigma-Aldrich) was added as an internal standard. The diluted sample was filtered using a PTFE syringe filter (0.2 µm pore size, Sigma-Aldrich) before injection.

*2.2.3.3. Two-dimensional heteronuclear single-quantum correlation NMR analyses.* The pyrolysis oils and hydrotreated-oils were also analyzed by two-dimensional (2D) $^{1}H$-$^{13}C$ heteronuclear single-quantum correlation NMR (2D HSQC-NMR) using methods described by Lancefield et al. [38]. A Bruker Ascend 700 MHz equipped with a CPP TCI probe or a 500 MHz spectrometer with a CPP BBO probe were used. The pyrolysis liquids and product oils were dissolved in DMSO-$d_6$ (10% w/w). The HSQC-NMR spectra (1024 points for $^{1}H$ or 256 points for $^{13}C$) were recorded using a 90° pulse angle, a 1.5 s relaxation delay, and 0.08 s acquisition time for a total of 48 scans.

*2.3. Experimental procedures*

*2.3.1. Fast pyrolysis experiments*

The pyrolysis experiments were performed in a mechanically stirred bed reactor filled with quartz sand (Fig. 1).

The microalgae were placed in the purging chamber (3) under constant nitrogen flow and then fed into the fast pyrolysis reactor at a rate of 1.67 g $min^{-1}$ via a screw feeder (2). Two fast pyrolysis temperatures (380 °C and 480 °C) were investigated, and experiments at each temperature setting were performed in triplicate. The mechanically stirred bed reactor is equipped with a mechanical stirrer (4) providing adequate mixing of the bed (i.e., quartz sand) and the biomass source. The nitrogen flow rate was set (1) at approximately 180 l $h^{-1}$ and fed from the bottom and the top of the reactor at approximately a 20-to-1 volumetric ratio. About 100 g of feedstock was fed into the reactor for each experiment within 1 h. The feeding screws are cooled to avoid thermal decomposition of the feed prior to feeding.

Pyrolytic vapors formed inside the reactor are transferred to a knock-out vessel (6) to capture any solid particles in the pyrolytic vapors. The knock-out vessel was maintained at 500 °C to avoid the premature condensation of the vapors. The pyrolysis vapors were initially cooled in an electrostatic precipitator (ESP) (7). The ESP wall temperature was maintained at 80 °C. The oil collected in the ESP is denoted as the heavy pyrolysis oil phase. Subsequently, the remaining vapors were cooled in two, serially connected downstream tap water cooled condensers (9). These condensed products are designated as the aqueous phase. After each experiment, the liquids were collected from the ESP collection flask, and the tap-water cooled condenser flasks, filtered and separated in case of the formation of two liquid phases.

The set-up is equipped with a cotton filter (10), to minimize any residual solid particles and vapor droplets entering the outlet gas flow meter (11). Reactor temperature, gas flow rates, and outlet gas temperature were monitored during each experiment.

After the fast pyrolysis reaction, four main products were formed, viz. two liquid phases (a heavy phase pyrolysis oil and an aqueous phase), solid residue (char) and a non-condensable gas phase. An overview of the procedure to separate the various products for mass balance calculations is given in Fig. 2.

Yields (% w/w) of each fast pyrolysis product were calculated on an as-received feedstock basis. Before and after each experiment, the ESP ($m_{ESP,\ initial}$ and $m_{ESP,\ final}$), the glass condenser flasks ($m_{cond,\ initial}$ and $m_{cond,\ final}$) and the cotton filter ($m_{filter,\ initial}$ and $m_{filter,\ final}$) (including the piping) were weighed. The heavy phase yield ($Y_{heavy}$) is based on the differences in mass of the ESP (before and after fast pyrolysis) added by the mass of heavy phase present in the condenser flasks ($m_{ow} - m_{wo}$), see Eq. (1) for details.

$$Y_{heavy} = [(m_{ESP,final} - m_{ESP,initial}) + (m_{filter,final} - m_{filter,initial}) + (m_{ow} - m_{wo})]. \frac{100}{m_f} \quad (1)$$

The aqueous phase yields ($Y_{aqueous}$) calculation is based on the mass differences of the two glass condenser flasks added by the amount of aqueous phase in the ESP ($m_{wo}$), as shown in Eq. (2).

$$Y_{aqueous} = [(m_{cond,final\_}m_{cond,initial}) + m_{wo}) - m_{ow}]. \frac{100}{m_f} \quad (2)$$

Pyrolytic char yields ($Y_{char}$) were determined by subjecting the collected solids (char and fluidized bed material) to loss on ignition (L.O.I.) analysis. This analysis measures the weight loss of a sample after ignition and combustion ($\Delta m_{cb}$) which was carried out in a muffle furnace (Carbolite AAF 1100) at 600 °C for a minimum of 6 h. Total char yield is the summation of the amount of char based on L.O.I. analyses, the suspended chars in the oil ($m_{co}$), chars in the knockout vessel ($m_{ck}$), chars that were taken for sample analysis ($m_{cs}$), and compensated with the ash content of the char ($A_c$), as given by Eq. (3).

$$Y_{char} = \left[\left(\frac{\Delta m_{cb}}{100\% - A_c}\right) + m_{co} + m_{ck} + m_{cs}\right]. \frac{100}{m_f} \quad (3)$$

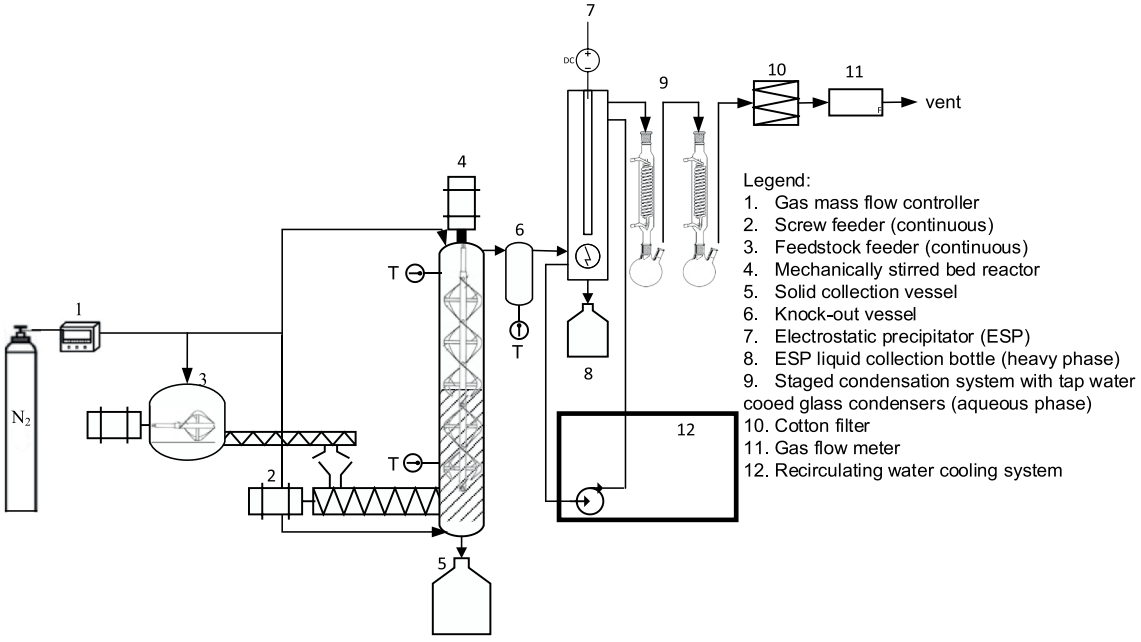


**Fig. 1.** Schematic representation of the fast pyrolysis set-up used in this study.

Fast pyrolysis non-condensable gas yield ($Y_{NCG}$) was calculated based on the difference between the average volumetric gas flow during biomass feeding ($\overline{Q_s}$) at the outlet of the pyrolysis system and the average nitrogen volumetric flow ($\overline{Q_b}$) introduced into the reactor (Eq. (4)). Conversion of the volumetric flow rates to mass flow rates was done by determining the gas density of the mixture ($\rho_{m,\,t}$). Considering the non-ideal nature of pyrolytic NCG, the density was calculated using the Peng-Robinson equation of state at gas outlet conditions and based on the NCG composition ($N_2$ free) as analyzed by the micro-GC. The calculations were performed using the Aspen® Hysis® software package.

$$Y_{NCG} = [(\overline{Q_s} - \overline{Q_b}).\, t.\, \rho_{m,t}].\, \frac{100}{m_f} \quad (4)$$

Mass balance closure was defined as the sum of the liquid yields (heavy phase and aqueous phase), char yield, and NCG yield (Eq. (5)).

$$Mass\ balance\ closure = Y_{heavy} + Y_{aqueous} + Y_{char} + Y_{NCG} \quad (5)$$

*2.3.2. Catalytic hydrotreatment reactions*

The catalytic hydrotreatment reactions were carried out in a stainless steel batch reactor (100 ml, Parr Instruments Co.) equipped with a Rushton-type turbine (agitation speed at 1000 rpm) as described in a previous study [37]. Temperature and pressure were monitored in real-time and logged on a computer.

Prior to each catalytic hydrotreatment, the reactor was filled with heavy phase pyrolysis oil (15 g), catalyst (0.75 g) and DMDS (25 µl). Initially, the reactor was flushed with hydrogen several times and then pressurized using hydrogen at room temperature for further leak testing. Leak testing was done by pressurizing the reactor to 15 MPa. Subsequently the pressure was reduced purposely to achieve an initial pressure of 10 MPa. The reactor was then heated to 350 °C at a heating rate of approximately 8 °C $min^{-1}$. The reaction time was started when the predetermined temperature was reached. The pressure at this stage was typically 14–15 MPa. Reactions were performed in a batch mode without the addition of hydrogen gas during reaction. The pressure and temperature values were recorded during the reactions, and the data were saved and displayed using a data logger and a PC. After 4 h

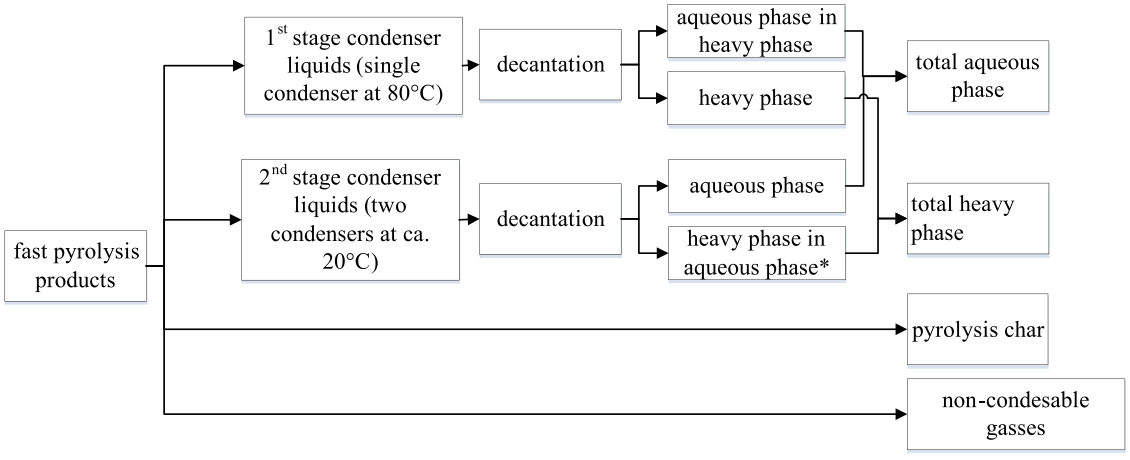


*heavy phase in aqueous phase was not used in chemical analyses

**Fig. 2.** Schematic representation of the workup procedure for fast pyrolysis products.

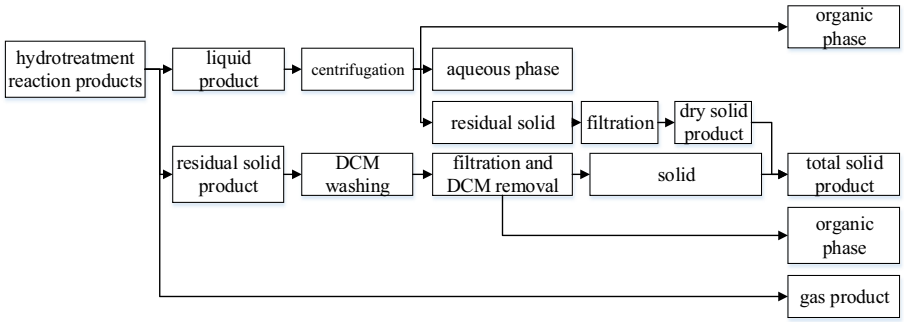


**Fig. 3.** Schematic representation of the workup procedure for the catalytic hydrotreatment reactions.

**Table 3**
Relevant compositional properties of the microalgae feed and the energy content.

| Strain | Ash (% w/w) | Elemental analysis (% w/w) | | | | | Lipids (% w/w) | Proteins (% w/w) | HHV (MJ $kg^{-1}$) |
|---|---|---|---|---|---|---|---|---|---|
| | | C | H | N | S | O | | | |
| NG | 12.4 | 48 | 8 | 7 | 1 | 25 | 13.4 | 32.2 | 23.1 |
| SA | 20 | 38 | 6 | 6 | 1 | 30 | 13.1 | 30 | 16.8 |

reaction time, the reactor was cooled to room temperature at a rate of about 10–15 °C $min^{-1}$. To affirm reproducibility and comparability of the hydrotreatment study results, experiments were carried out in duplicates.

After the catalytic hydrotreatment reaction, four main products were produced, viz. two liquid phases (an organic and an aqueous phase), solid residue (chars and catalyst residues) and a non-condensable gas phase. An overview of the procedure to separate the various products for mass balance calculations is given in Fig. 3.

The yield of each catalytic hydrotreatment product was calculated on a pyrolysis oil intake basis. After the hydrotreatment reaction and depressurization of the reactor, the gas phase was collected in a three-liter Tedlar gas bag. The gas sample was further analyzed using GC-TCD to determine its composition. The liquid and solid products were taken from the reactor and transferred to a 15 ml centrifuge tube (Sigma-Aldrich) and then centrifuged at 4500 rpm for 15 min. The hydrotreated liquid phase consists of an organic phase (lighter-than-water) and an aqueous phase. The liquid phases were separated by decantation and weighed for mass balance calculations. The solids in the centrifuge tube were washed with dichloromethane (DCM, Sigma-Aldrich) and then filtered using a filter paper with known weight and left to dry overnight.

The cooled reactor was flushed with DCM to remove residual oils and solids on the reactor wall and bottom. The resulting mixture was filtered using a filter paper with known weight and dried at room temperature overnight to collect the solids. The two DCM washing liquids were combined, and the DCM was removed by evaporation at room temperature. The remaining organic fraction was weighed and added to the organic phase obtained after the reaction ($m_{HDO,\ oil}$). The measured weights of the organic phase, aqueous phase ($m_{HDO,\ aqueous}$), and the combined solid products ($m_{HDO,\ solid}$) were used for product yield calculations (% w/w) (Eqs. (6)–(9)). The gas yield was calculated from the mass balance differences.

$$Y_{HDO-oil} = \frac{m_{HDO,oil}}{Mass\ of\ pyrolysis\ oil\ feed} \times 100 \quad (6)$$

$$Y_{HDO-aq} = \frac{m_{HDO,aqueous}}{Mass\ of\ pyrolysis\ oil\ feed} \times 100 \quad (7)$$

$$Y_{HDO-char} = \frac{m_{HDO,solid}}{Mass\ of\ pyrolysis\ oil\ feed} \times 100 \quad (8)$$

$$Mass\ balance = \frac{\sum (mass\ of\ product\ (s))}{Mass\ of\ pyrolysis\ oil\ feed} \times 100 \quad (9)$$

## 3. Results and discussion

### 3.1. Feedstock characterization

The two algae feeds used in this study were pre-dried and shaped (ground and sieved) into 2–3 mm flakes-like particles before use as a pyrolysis feed. Relevant properties (ash content, elemental composition, lipid, protein, and energy content) were determined and reported earlier by López Barreiro et al. [39], and the data are summarized in Table 3. The oxygen content of both feeds is between 25 and 30% w/w, and the carbon content between 38 and 48% w/w. The carbon and oxygen contents for both feeds are in the range reported in the literature for *Scenedesmus* sp. and *Nannochloropsis oculata* ([2,5]). Both contain considerable amounts of ash (12.4–20% w/w). The carbon content is highest for NG (48% w/w), and combined with the lower ash content this leads to a substantially higher HHV than for SA (23.1 MJ $kg^{-1}$ for NG and 16.8 MJ $kg^{-1}$ for SA) [40]. The lipid and protein fraction in both feedstocks are about similar (13.1–13.4% w/w lipids and 30–32.2% w/w proteins). The protein content is in the range reported in the literature, whereas the lipid content is considerably lower compared to other microalgae (up to 50–70% w/w) [41–44]. This is likely due to differences in cultivation media, cultivation techniques, and processing parameters [45–47].

Thermogravimetric analysis (TGA) under an $N_2$ atmosphere was performed to determine the thermal degradation behavior of both microalgae, which is amongst others of relevance to determine the optimum pyrolysis temperature (Fig. 4). Mass loss of the feedstock started at temperatures below 100 °C, due to evaporation of residual water and possibly also some dehydration reactions. Devolatilization of the organic matter in the microalgae feedstock was observed in the temperature range between 130 and 500 °C and is likely associated with decomposition/volatilization of lipids, carbohydrates, and proteins [48–51]. The TGA data are in line with those reported by Lopez-Gonzalez et al. [14] for *Scenedesmus almeriensis* and *Nannochloropsis gaditana* microalgae. Wang et al. [19] reported TGA data for *Nannochloropsis* microalgae as well those for isolated fractions thereof (lipids, proteins and carbohydrates). The main decomposition temperature zone was between 200 and 450 °C, and the pyrolysis TGA peak for the

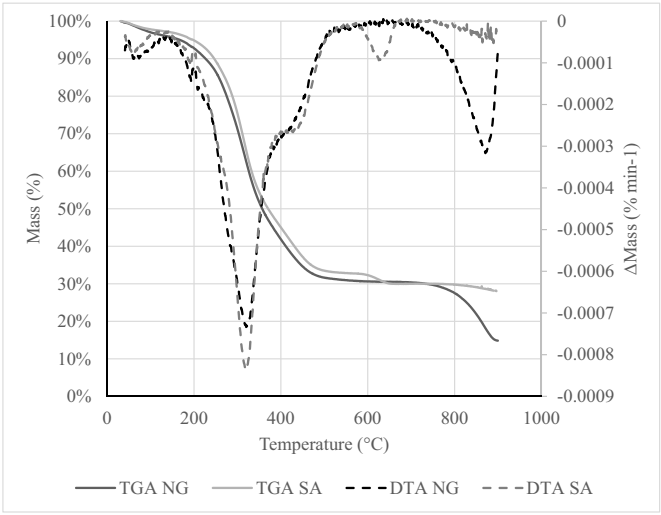


**Fig. 4.** TGA–DTG curves of NG and SA under nitrogen flow. DTG curve was manually calculated from TGA data and smoothed using a moving average.

microalgae was found at 317 °C. Our data are in line with these findings. For the individual, isolated fractions, maximum pyrolysis peaks were found at 353 °C (lipids), 310 °C (proteins) and 275 °C (carbohydrates). As such, we can conclude that pyrolysis temperatures > 450 °C will be required to pyrolyze the most relevant fractions of the microalgae.

The slight loss of mass at high temperatures (> 600 °C) in both feedstocks is not caused by volatilization of organic material but most likely by the thermal decomposition of metal oxide components present in the ash of the feedstock (Supplementary Table S1), which can be significant [52]. For instance, NG ash is high in calcium salts and these are known to decompose at about 800 °C, while SA contains substantial amounts of iron, manganese, and magnesium salts that have reported to decompose at lower temperatures (ca. 600 °C).

### 3.2. Fast pyrolysis experiments

The fast pyrolysis experiments were carried using pre-dried microalgae in a mechanically stirred fluidized bed reactor with fractional condensation. This resulted in two oil fractions: a heavy oil collected at 80 °C and an aqueous phase obtained at room temperature. The heavy phase pyrolysis oils produced at 380 °C were assigned as $FP_{380}$ (SA $FP_{380}$ and NG $FP_{380}$), while the heavy phase pyrolysis oils obtained at 480 °C were assigned as $FP_{480}$ (SA $FP_{480}$ and NG $FP_{480}$). A comparison of the fast pyrolysis product yields for the two feedstocks pyrolyzed at 380 °C and 480 °C are presented in Table 4. The heavy phase pyrolytic oil yields were between 20 and 31% w/w. The highest yield was obtained using NG at 480 °C. The feed has a significant effect on the product yields (except the aqueous phase yield) and higher heavy pyrolysis oil yields were obtained for NG, irrespective of the pyrolysis temperature (based on statistical analyses of the data, *t*-tests). A likely explanation is the lower ash content and higher carbon content of the latter feed (Table 3).

**Table 5**
Product yields for the catalytic hydrotreatment experiments on pyrolysis feed basis[a].

| Fast-pyrolysis feed | Product yields (% w/w) | | | |
|---|---|---|---|---|
| | Organic | Aqueous | Solid | Gas[b] |
| NG $FP_{380}$ | 53.3 ± 1.2 | 0.7 ± 0.1 | 5.0 ± 0.4 | 41.1 ± 1.6 |
| NG $FP_{480}$ | 56.1 ± 2.4 | 1.0 ± 0.1 | 6.8 ± 0.3 | 36.1 ± 2.7 |
| SA $FP_{380}$ | 57.2 ± 4.1 | 3.0 ± 1.4 | 4.6 ± 1.2 | 35.3 ± 4.3 |
| SA $FP_{480}$ | 52.7 ± 3.1 | 13.4 ± 3.6 | 5.6 ± 1.8 | 28.4 ± 1.3 |

[a] Duplicate experiments.
[b] Based on difference.

The non-condensable fast pyrolysis gases (NCGs) consist mainly of $CO_2$ and CO (see Supplementary information, Table S2). In addition, 6–25% v/v of light hydrocarbons were present in the gas-phase. At higher fast pyrolysis temperatures, gas production was increased considerably at the expense of char, likely due to higher levels of thermal cracking and devolatilization. The gas composition also is a function of temperature, with higher temperatures resulting in additional hydrogen and light hydrocarbons formation at the expense of $CO_2$.

### 3.3. Catalytic hydrotreatments

The heavy phase pyrolysis oils obtained from the two microalgae species at two- fast pyrolysis temperatures were subjected to a catalytic hydrotreatment. The hydrotreated product oils are abbreviated according to the microalgae species and pyrolysis temperatures (e.g., SA $HDO_{380}$ or NG $HDO_{480}$). The product yields for the catalytic hydrotreatment reactions are given in Table 5. Typically, 4 product phases are obtained, an organic liquid phase, an aqueous phase, solids, and gas-phase components. The amounts of solid products (5–7% w/w) and hydrotreated pyrolysis oils (organic phases, 53–57% w/w) after catalytic hydrotreatment were within very narrow ranges. The yields of the aqueous phase after hydrotreatment the SA heavy phase pyrolysis oils were significantly higher (at both temperatures) than the yield when using the NG oil as the feed (based on statistical analyses, *t*-test). The hydrotreated oils showed a low viscosity, indicating a reduction of the average molecular weight of the (oligomeric) compounds during hydrotreatment (see below). This is in contrast to the heavy phase pyrolysis oil feeds for the catalytic hydrotreatment, which were highly viscous.

Our oil yields (between 53 and 57%) are considerably lower than those reported by Duan (ca. 70% w/w) [53], though it is not possible to substantiate this conclusions by statistical analyses as replicate experiments are not reported in ref. [53] The most likely explanation for this observation is the fact that Duan used a *Nannochloropsis* sp. derived biocrude from a hydrothermal liquefaction (HTL) process, which is known to give oils with different chemical compositions than those obtained from pyrolysis processes. In addition, Duan used palladium on carbon (5% Pd) at a higher catalyst loading and applied longer reaction times, which will also affect oil yields and composition. Another

**Table 4**
Product yields for fast pyrolysis with staged condensation of two microalgae species at different temperatures[a].

| Strain | Fast pyrolysis temperature (°C) | Product yield (% w/w based on feed) | | | | Total |
|---|---|---|---|---|---|---|
| | | Heavy phase | Aqueous phase | Gas | Solids | |
| NG | 380 | 24.6 ± 1.0 | 11.6 ± 1.6 | 14.3 ± 1.9 | 49.3 ± 2.5 | 99.8 ± 3.7 |
| | 480 | 31.2 ± 3.0 | 11.6 ± 1.4 | 23.4 ± 2.3 | 25.1 ± 2.4 | 91.3 ± 4.7 |
| SA | 380 | 20.3 ± 0.4 | 13.5 ± 0.8 | 7.2 ± 1.1 | 43.9 ± 1.2 | 85.0 ± 1.9 |
| | 480 | 20.3 ± 2.9 | 13.2 ± 0.9 | 14.6 ± 3.8 | 41.8 ± 3.8 | 90.0 ± 1.4 |

[a] At least triplicate experiments, standard deviation is given.

**Table 6**
Properties of the heavy phase pyrolysis oils and catalytic hydrotreatment products[a].

| Heavy phase pyrolysis oils | Elemental composition (% w/w) | | | | HHV (MJ $kg^{-1}$) |
|---|---|---|---|---|---|
| | Carbon | Hydrogen | Nitrogen | Oxygen | |
| NG $FP_{380}$ | 64.9 ± 0.8 | 9.6 ± 0.1 | 7.2 ± 0.4 | 15.9 ± 2.1 | 31.1 ± 0.8 |
| NG $FP_{480}$ | 64.9 ± 2.3 | 8.9 ± 0.5 | 8.6 ± 0.3 | 13.6 ± 1.2 | 32.4 ± 1.1 |
| SA $FP_{380}$ | 64.0 ± 1.5 | 9.0 ± 0.1 | 11.0 ± 0.3 | 19.1 ± 1.0 | 29.0 ± 0.7 |
| SA $FP_{480}$ | 66.2 ± 1.8 | 8.9 ± 0.3 | 10.7 ± 0.7 | 13.6 ± 0.8 | 31 ± 0.8 |
| Hydrotreated oils | Elemental composition (% w/w) | | | | HHV (MJ $kg^{-1}$) |
| | Carbon | Hydrogen | Nitrogen | Oxygen | |
| NG $HDO_{380}$ | 79.5 ± 0.4 | 12.0 ± 0.1 | 7.0 ± 0.1 | 1.6 ± 0.4 | 37.3 ± 0.3 |
| NG $HDO_{480}$ | 80.5 ± 0.8 | 11.5 ± 0.2 | 6.0 ± 0.6 | 2.0 ± 1.6 | 41.7 ± 0.6 |
| SA $HDO_{380}$ | 79.6 ± 0.2 | 12.0 ± 0.1 | 6.7 ± 0.4 | 1.8 ± 0.1 | 41.9 ± 0.2 |
| SA $HDO_{480}$ | 78.2 ± 0.9 | 11.0 ± 0.1 | 6.4 ± 0.7 | 4.2 ± 1.5 | 39.9 ± 0.3 |

[a] Average value based on duplicate analyses, on as produced basis.

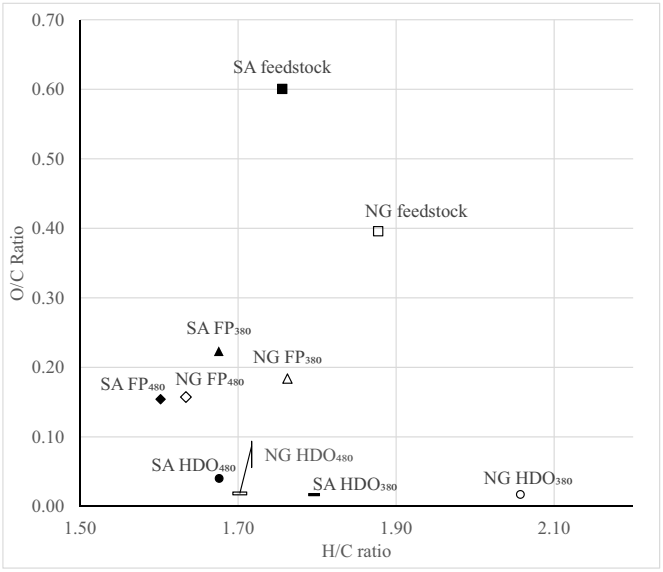


**Fig. 5.** Van Krevelen diagram for heavy phase fast pyrolysis oils and hydrotreated oils for the two microalgae feeds.

hydrotreatment study used a *Nannochloropsis salina* oil obtained by extraction instead of pyrolysis, which was hydrotreated over a reduced pre-sulphided NiMo/$\gamma$-$Al_2O_3$ catalyst (7 h, 360 °C and 500 psig $H_2$ pressure [54]). High conversion (98.7% w/w) to an organic liquid containing 56.2% of $C_{20}$ hydrocarbons was reported. These high yields are likely due to the high lipid content of this feed.

### 3.4. Elemental balances and energy contents of fast-pyrolysis and hydrotreated oils

Fast pyrolysis and catalytic hydrotreatment have a major impact on the elemental composition of feeds/products. In Table 6, the elemental composition and energy content of the heavy phase pyrolytic oils from fast pyrolysis and the hydrotreated oils are provided. The heavy phase fast pyrolysis oils contain approximately 65% w/w carbon and a considerable amount of bound oxygen (13–19% w/w). Higher fast pyrolysis temperatures did not affect the carbon content in the heavy phase pyrolysis oil significantly for both microalgae species. However, the amount of oxygen (as oxygenates) is a strong function of the fast pyrolysis temperature, with higher temperatures leading to pyrolysis oils containing less oxygen. This decrease in oxygen content coupled with an increase in the amount of water, implies that condensation/dehydration reactions are favored at high pyrolysis temperatures. Similar temperature effects on product composition were observed for the pyrolysis of *Chlorella vulgaris* [16] and *Dunaliella salina* [15]. The nitrogen content in the heavy phase pyrolysis oils (7.2–11.0% w/w, Table 6) is in the range as reported for pyrolysis liquids from microalgae (6.5–10.8% w/w, see Table 1 for details).

Upon catalytic hydrotreatment, the carbon content of the product oil increased from on average 65% w/w to 80% w/w. The oxygen content is considerably reduced (70–90%), and hydrotreated oils with oxygen contents as low as 1.6% w/w were successfully obtained. This high level of oxygen removal is indicative of a high rate of hydrodeoxygenation reactions. All effects are illustrated in a van Krevelen plot given in Fig. 5.

The nitrogen contents of the pyrolysis oils are higher than reported for wood-derived pyrolysis oils [55]. This is due to the high amounts of proteins in the feedstock, which are converted to amongst others small nitrogen-containing molecules during pyrolysis [1]. SA derived pyrolysis oils contain significantly more nitrogen compared to NG derived ones (statistical analyses, *t*-tests), which is surprising due to the lower protein content of SA (Table 3). Apparently, not only the amount but also other properties of the proteins (e.g. composition) play a role. After hydrotreatment, the nitrogen content in the product oils is significantly reduced (statistical analyses, t-tests, the only exception is the NG oil hydrotreated at 380 °C), though still above 6% w/w in all cases. This implies that hydrodenitrification reactions only occur to a limited extent. A possible explanation is the nature of the organo-nitrogen

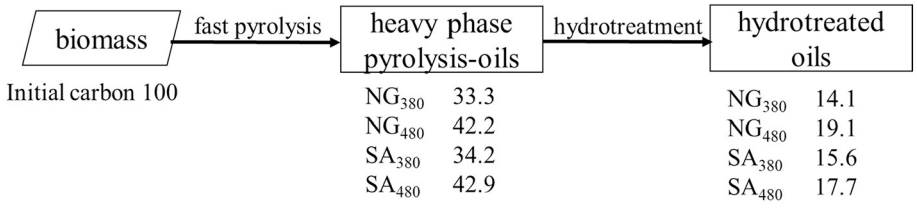


**Fig. 6.** Carbon balances from two-step fast pyrolysis and hydrotreatment reactions.

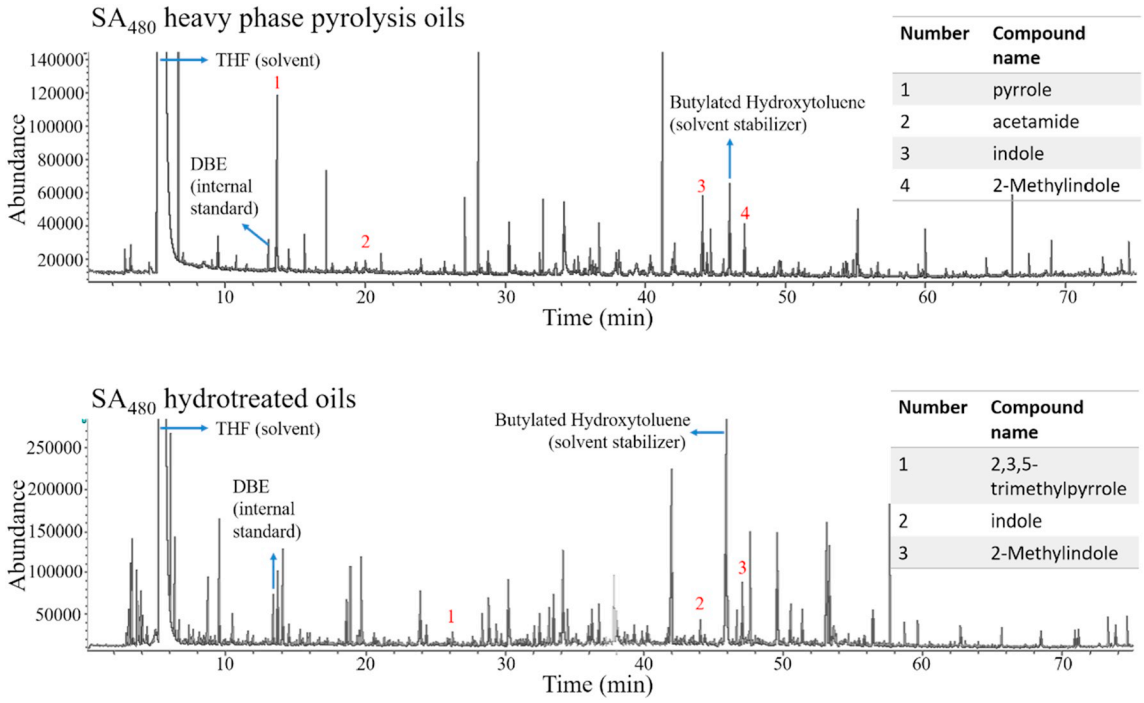


**Fig. 7.** GC–MS chromatogram for a representative pyrolysis oil and the corresponding hydrotreated oil ($SA_{480}$).

**Table 7**
GC × GC-FID quantification of chemicals groups found on heavy phase pyrolysis oils and hydrotreated oils.

| Heavy phase pyrolysis oils | | | | |
|---|---|---|---|---|
| Group | NG (% w/w on oil) | | SA (% w/w on oil) | |
| | 380 °C | 480 °C | 380 °C | 480 °C |
| Cycloalkanes | 0.05 | 0.07 | 0.06 | 0.06 |
| Alkanes | 1.82 | 1.43 | 2.42 | 1.74 |
| Non-oxygenated aromatics | 0.63 | 0.59 | 1.28 | 0.62 |
| Naphthalenes | 0.32 | 0.45 | 0.31 | 0.38 |
| Ketones, acids, and alcohols | 7.15 | 6.42 | 6.64 | 5.83 |
| Phenolics | | | | |
| Methoxy-substituted phenolics | 5.37 | 4.84 | 6.00 | 5.45 |
| Alkylphenolics/catechols | 4.8 | 6.57 | 3.95 | 6.68 |
| Total volatile fraction of oil | 20.14 | 20.37 | 20.66 | 20.76 |

| Hydrotreated oils | | | | |
|---|---|---|---|---|
| Group type | NG (% w/w on oil) | | SA (% w/w on oil) | |
| | 380 °C | 480 °C | 380 °C | 480 °C |
| Cycloalkanes | 0.7 | 0.91 | 0.89 | 3.86 |
| Alkanes | 14.23 | 11.35 | 9.03 | 14.37 |
| Non-oxygenated aromatics | 3.67 | 5.92 | 3.92 | 9.21 |
| Naphtalenes | 0.74 | 2.29 | 0.7 | 4.76 |
| Ketones, acids, and alcohols | 1.3 | 1.61 | 2 | 1.71 |
| Phenolics | | | | |
| Methoxy-substituted phenolics | 2.73 | 4.01 | 4.62 | 7.38 |
| Alkylphenolics/catechols | 5.32 | 7.54 | 4.01 | 12.85 |
| Total volatile fraction of oil | 28.69 | 33.63 | 25.17 | 54.14 |

compounds present. It is well known that particularly aromatic nitrogen-containing molecules like substituted indoles, which were indeed detected in the product oils (see below), are difficult to remove by a catalytic hydrotreatment [56].

The energy content of the hydrotreated products (37.3–41.9 MJ $kg^{-1}$) is by far higher than that of the intermediate pyrolysis oil (29–32.4 MJ $kg^{-1}$) and the microalgae feed (16.8–23.1 MJ $kg^{-1}$) due to substantial removal of bound oxygen by the catalytic hydrotreatment process.

### 3.4.1. Overall carbon balances

Fig. 6 summarizes the overall carbon balances for the two-step fast-pyrolysis/hydrotreatment of microalgae, as reported in this paper. Overall carbon yields for the two-step process are between 14.1 and 19.1% w/w. Best results were obtained for the NG feed at 480 °C (19.1% w/w). Fast-pyrolysis is best performed at 480 °C, and 33.3–42.9% w/w of the carbon in the microalgae feed is retained in the heavy phase pyrolysis-oils. Yields are lower at 380 °C, due to the formation of larger amounts of char.

## 3.5. Chemical composition of the fast pyrolysis and hydrotreated oils

A wide range of analyses was performed to determine the molecular composition of the heavy phase pyrolysis oils and hydrotreated-oils. These include GC–MS, GC × GC-FID, and two-dimensional NMR (2D HSQC-NMR).

### 3.5.1. GC analyses of heavy phase pyrolysis oils and hydrotreated oils

GC–MS analyses for the intermediate pyrolysis oils and hydrotreated products were performed to gain insights into the low molecular weight components present in oils and the molecular transformations occurring during hydrotreatment. A representative example of a GC–MS chromatogram is given in Fig. 7, those for other product classes are given in the Supplementary information (Figs. S3 and S4).

Semi-quantification of the data was done using relative peaks areas (see Tables S3–S10). The individual components were categorized according to their chemical structures viz: alkanes and alkenes, non-oxygenated aromatics, phenolics, fatty acids and esters, fatty alcohols and nitrogen containing compounds. The pyrolysis oils contain typical components belonging to the alkane/alkene group (e.g. hexadecene, derived from the lipid fraction in the microalgae), N-containing compounds (e.g. indoles and pyrrolidinones, derived from the protein fraction), carboxylic acids (e.g. acetic acid, from the carbohydrate fraction) and phenolics. The composition changed after hydrotreatment and the hydrotreated oils of both microalgae showed the presence of

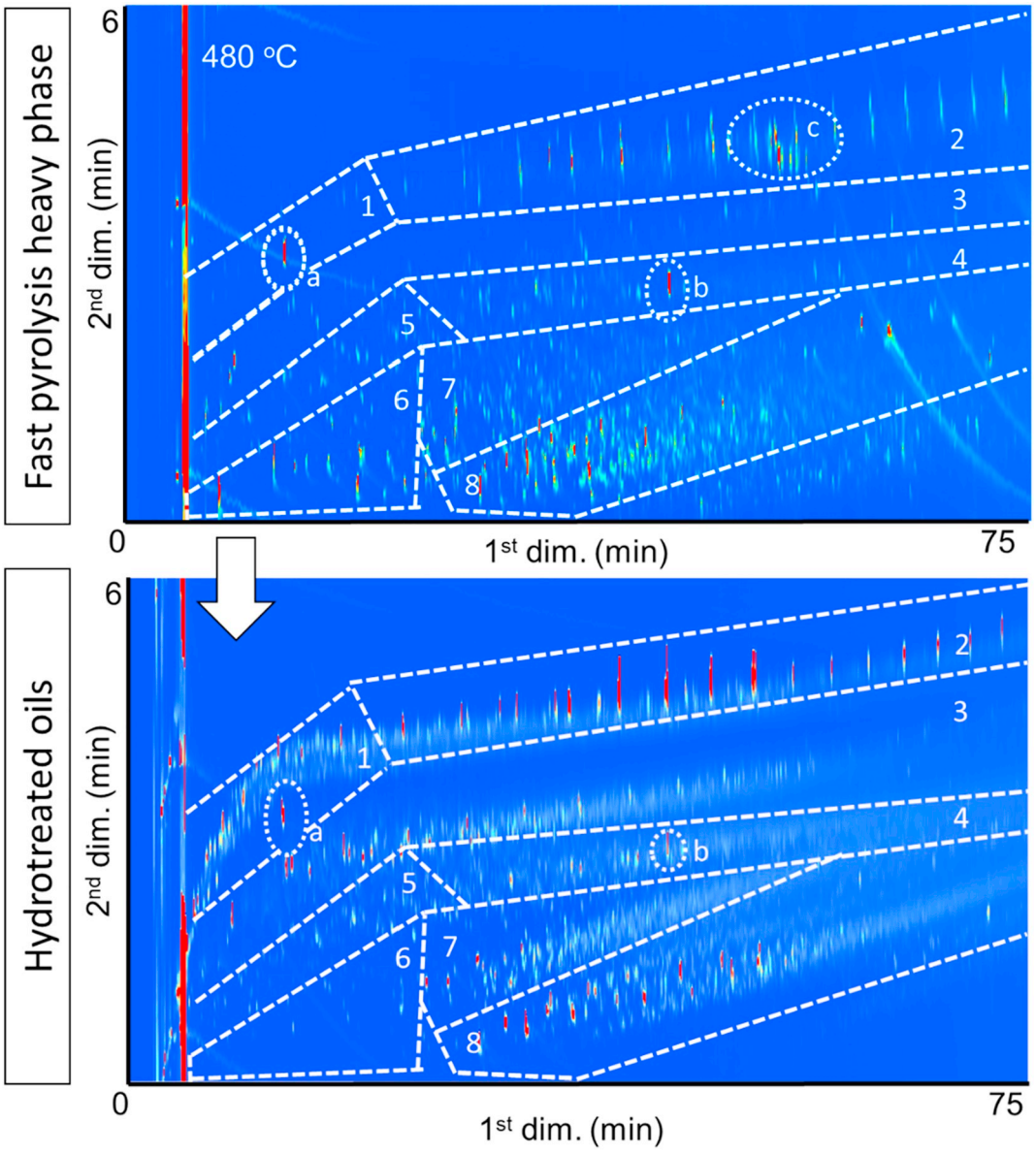


**Fig. 8.** Representative GC × GC-FID analyses of a heavy phase pyrolysis oil and a corresponding hydrotreated oil ($SA_{480}$). Region 1: cyclic alkanes; region 2: primarily linear/branched alkanes; regions 3 and 4: non-oxygenated aromatics (including polycyclic aromatic hydrocarbons); regions 5 and 6: oxygenates (e.g., ketones, alcohols, and acids), region 7: methoxy-substituted phenolics, and region 8: alkylphenolics and catecholics "a" is internal standard (n-dibutyl ether), and "b" is butylated hydroxytoluene (stabilizer in THF).

saturated hydrocarbons (e.g., hexadecane), aromatics (e.g., toluene, propylbenzene) and phenolics (e.g., 4-methylphenol and phenol). After catalytic hydrotreatment, most of the nitrogen containing heterocycles are still present, indicating that these compounds are difficult to remove by this treatment, in line with literature data [4,21].

To quantify the amounts of the main organic compound classes (aromatics, phenolics, alkanes, etc.), the heavy phase pyrolysis oils and hydrotreated oils were analyzed using GC × GC-FID (Table 7, Fig. 8, see also Supplementary information, Figs. S1 and S2). Though nitrogen-containing compounds are present according to GC–MS, these were not calibrated in the GC × GC measurements and thus could not be quantified. The GC detectable components were categorized in eight distinct regions, see Fig. 8 for a representative example.

The heavy phase pyrolysis oils and hydrotreated oils from both microalgae display a wide range of compounds belonging to various product classes, in line with the GC–MS data (cyclic and linear/branched alkanes, non-oxygenated aromatics (including polycyclic aromatic hydrocarbons), light oxygenates (e.g., ketones, alcohols, and acids) and phenolic compounds (methoxy substituted phenolics, alkylphenolics, catechols)).

GC × GC reveals that the main component groups in the heavy pyrolysis oils are light oxygenates like ketones, acids and alcohols (derived from the cellulose fraction in the algae feed) and phenolics in the form of alkylphenolics/catechols and methoxy substituted phenolics. The hydrotreated oils contain mainly alkanes, non-oxygenated aromatics and phenolics. As such, the light oxygenates are predominantly converted during the hydrotreatment reaction to hydrocarbons. This is also expected based on the chemistry associated with hydrotreatment, viz. the conversion of oxygenates to hydrocarbons in the form of alkanes and aromatics [57], and in line with the GC–MS data.

The chromatograms for the hydrotreated oils also clearly show the typical products derived from the lipid fraction of the algae feed in region 2 in the form of linear and branched alkanes (e.g. hexadecane, pentadecane). Lipids are known to be converted to the individual fatty acids and esters and hydrocarbons in the pyrolysis step [19]. These

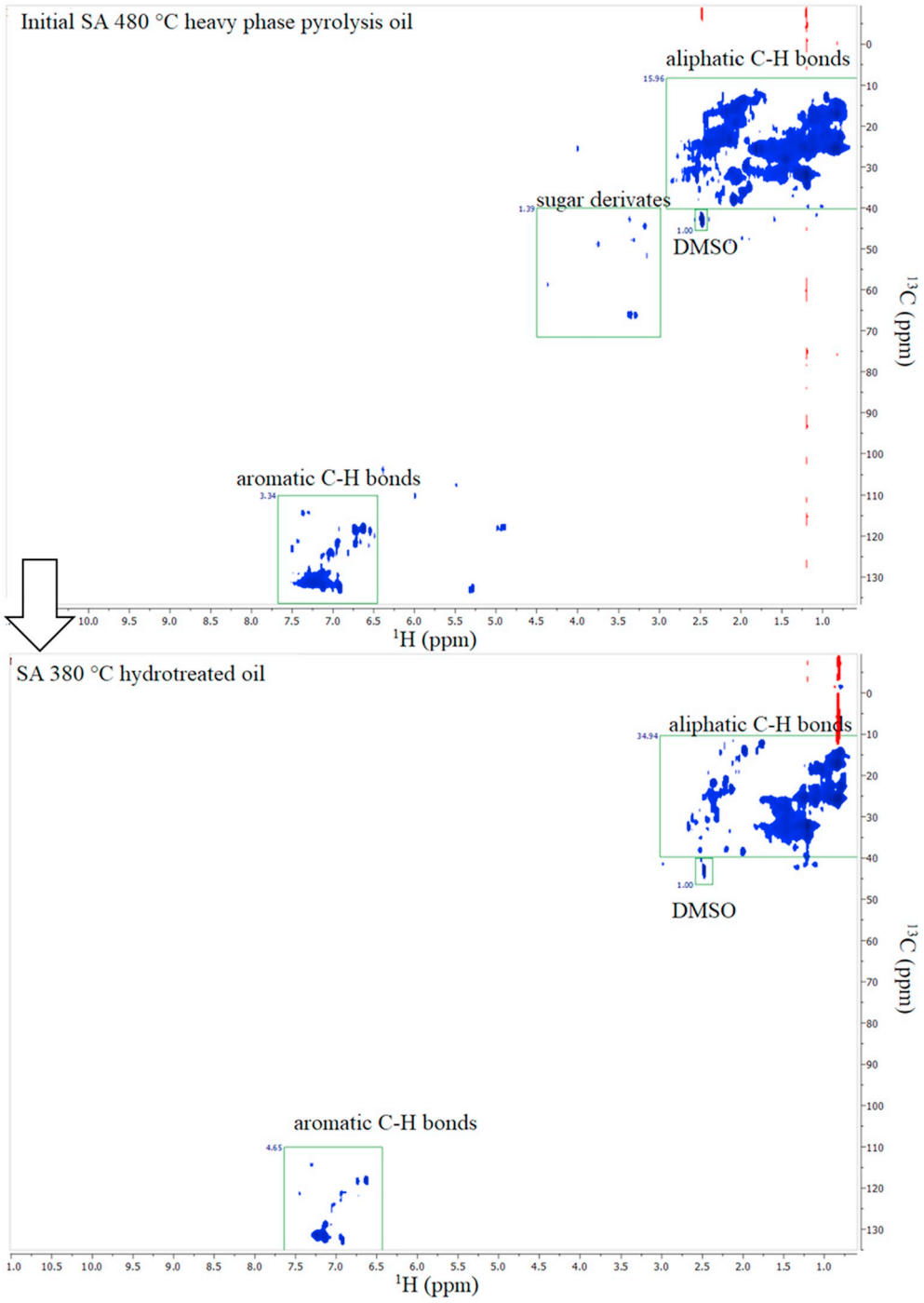


**Fig. 9.** Representative 2D-HSQC-NMR analyses of a representative heavy phase pyrolysis oil (SA 480, top) and the corresponding hydrotreated oil (bottom). DMSO is the solvent.

primary pyrolysis products are subsequently transformed to hydrocarbons in the hydrotreatment step by additional decarbonylation, decarboxylation as well as hydro(deoxy-)genation reactions [19].

Also of interest is the observation that the volatile fraction of the hydrotreated oils considerably higher than that of the pyrolysis oils. For example for SA, it is a factor of 2.5 higher when the hydrotreatment is performed at 480 °C. These findings indicate the occurrence of hydrocracking reactions during the hydrotreatment process, leading to a considerable reduction in molecular weight and thus a considerably higher amount of volatile, GC detectable compounds in the product oils. These findings are in line with literature data on the hydrotreatment of pyrolysis liquids [26,27,29].

Finally, the oils were characterized using 2D-NMR, which gives not only insights in the chemical composition of the GC detectables but also on that of the higher molecular weight fraction (Fig. 9 and Supplementary information, Figs. S5 and S6). HSQC-NMR analyses of pyrolysis oils instead of traditional 1-dimensional $^{1}$H and $^{13}$C NMR has two main advantages, viz. i) the overlapping peaks, occurring to a large extent when hundreds of components are present in the product, are reduced due to spreading of the signals into two dimensions and ii) a higher sensitivity and iii) shorter relaxation times. $^{1}$H-$^{13}$C-HSQC NMR provides a 2-D plot, with on one axis the $^{1}$H NMR shift and the $^{13}$C NMR shift on the other axis. Every peak is associated with a particular C-H unit in a certain chemical environment. Ben and Ragauskas [58] used

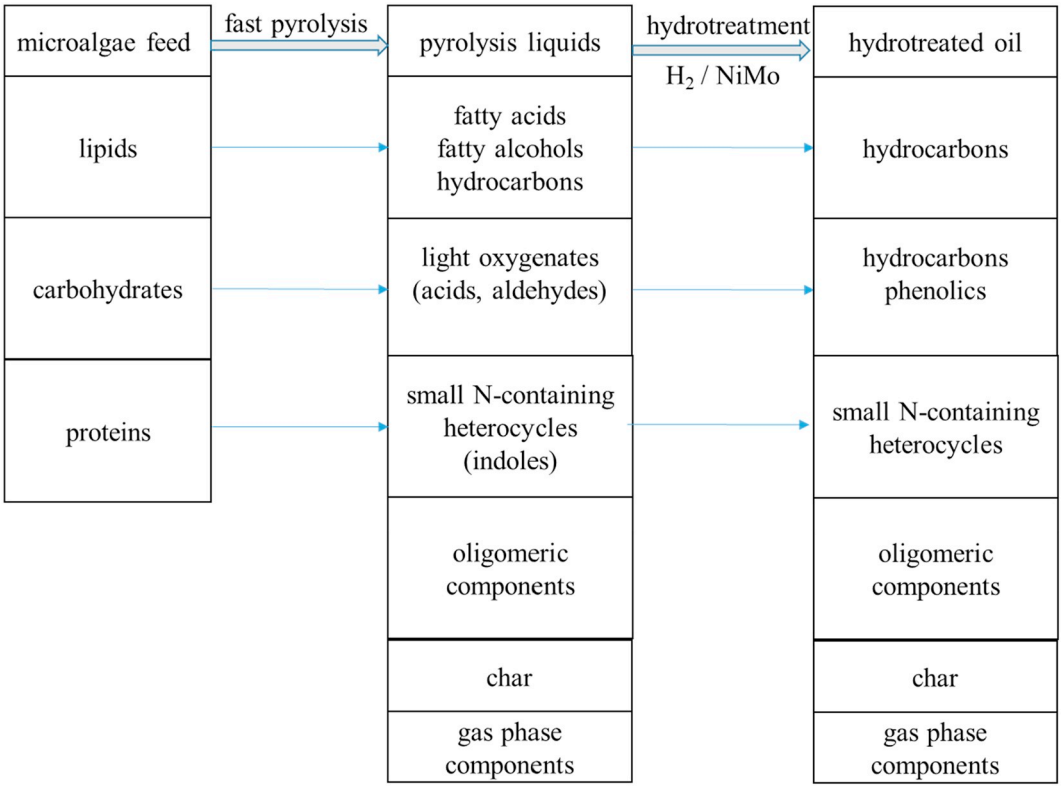


**Fig. 10.** Overview of major chemical transformations occurring during fast-pyrolysis and hydrotreatment of NG and SA.

this NMR method to characterize pyrolysis oils derived from the slow pyrolysis of lignin, cellulose and pine wood. A number of relevant regions were assigned belonging to different C-H bonds, viz: i) aromatic C-H bonds belonging to amongst others substituted phenolics (105–140 ppm in the $^{13}$C NMR dimension and 5.5–7.5 in the $^{1}$H NMR dimension, ii) methoxy groups (54–57 ppm in the $^{13}$C NMR dimension and 3.7–3.9 ppm in the $^{1}$H NMR dimension), and aliphatic C-H bonds (5–40 ppm in the $^{13}$C NMR dimension and 0.7–2.8 in the $^{1}$H NMR domain). Assignment of the C-H bonds of pyrolytic sugars, the collective term of sugar derivatives in pyrolysis oils from the conversion of the cellulose/hemi-cellulose fraction in the biomass feed, in HSQC NMR spectra were recently provided by Yu et al. [59]. These are typically present in the 5.5–2.5 ppm region in the $^{1}$H NMR dimension and 50–110 ppm range in the $^{13}$C NMR dimension.

The heavy phase pyrolysis oil from SA, obtained at 480 °C, shows the presence of aliphatic and aromatic C-H bonds (Fig. 9, top), in line with the GC × GC data. In addition, peaks are present in the pyrolytic sugar region, as a result of the presence of sugar derivatives (light oxygenates, like aldehydes, as well as oligomeric sugars). The HSQC-NMR of the hydrotreated product oil shows only two main regions, aliphatic and aromatic C-H bonds, and pyrolytic sugar peaks are absent. These findings are in line with the GC × GC data, showing a dramatic increase in alkanes and non-oxygenated aromatics upon catalytic hydrotreatment of the pyrolysis oils at the expense of light oxygenates.

### 3.6. Reaction network

Analyses of the chemical composition of the heavy pyrolysis oils as well as the hydrotreated oils by GC and NMR has provided relevant information on the major chemical transformations occurring in the pyrolysis and hydrotreatment steps in the two step sequence from micro-algae to product oils (see Section 3.5). A summary with emphasis on the conversions of the individual microalgae fractions (lipids, carbohydrates and proteins) is provided in Fig. 10.

## 4. Possible applications of the hydrotreated microalgae-oils

It has been shown that pyrolysis followed by catalytic hydrotreatment leads to hydrocarbon-rich oils with significantly lower oxygen contents (< 4.2% w/w) than the original microalgae feed (25–30% w/w). However, the oils as such are not yet suitable to serve as transportation fuels or as co-feeds for FCC units [60]. The major issues are the presence of organic nitrogen-containing compounds (6–7% w/w) and alkylphenolics. For both applications, stringent norms regarding the nitrogen content need to be fulfilled. A possible solution is a deep catalytic hydrodenitrification procedure, though this is likely to be very cumbersome, as the nitrogen-containing compounds in the products are mainly aromatic in nature (GC, e.g., substituted indoles), which are difficult to remove by standard hydrotreatment procedures and require dedicated catalysts [56].

Another possible approach to reduce the nitrogen content in the final product oils is to develop efficient separation procedures like (reactive) solvent extractions [64] for removal of organo-nitrogen components in pyrolysis oils. An additional advantage of this approach is that some of the N-heterocyclic compounds (e.g., indole and pyridine) have a market price considerably higher than that of (transportation) fuels [61,62]. As such, the separated nitrogen compounds could be further purified for use as bulk chemicals, while the hydrocarbon fraction could be used as a transportation fuel or co-fed to oil refineries.

## 5. Conclusions

This study shows that both marine microalga *Nannochloropsis gaditana* and freshwater microalga *Scenedesmus almeriensis* in dried form can be used as feedstock for fast pyrolysis processes. The temperature has a strong effect on the product yields and a higher fast pyrolysis temperature leads to a higher yield of heavy phase pyrolysis oils with lower oxygen contents. In addition, the heavy phase pyrolysis oil yields are also a function of the microalgae feed and the best results were obtained for NG (31.2% w/w). Catalytic hydrotreatment of the produced

heavy phase pyrolysis oils leads to a considerable improvement in the quality of the liquids. These were shown to be enriched in aromatics and hydrocarbons and have a considerably lower oxygen content (1.6–4.2% w/w) compared to the microalgae feeds (25–30% w/w). The overall carbon yield for the liquid product was approximately 15.6–19.1% w/w (based on the initial carbon content of the feedstock). The best results were obtained for the NG feed. A major issue is the presence of nitrogen heterocycles in the product oils, due to the presence of proteins in the feed. For further applications, upgrading will be required, e.g. by deep hydrodenitrification (HDN) of nitrogen-containing compounds (N-heterocyclic compounds viz. indole and pyridine) using dedicated catalyst or separation of the N-heterocyclic compounds from the product oils for chemical production using for instance advanced liquid-liquid extractions.

## Author statement

Neil Priharto: Validation, investigation, writing, visualization
Frederik Ronsse: conceptualization, methodology, resources, data curation, writing, review and editing
Wolter Prins: conceptualization, methodology, resources, writing, review and editing, supervision, funding acquisition
Robert Carleer: methodology, validation, resources, writing, review and editing
Hero Jan Heeres: conceptualization, methodology, validation, resources, data curation, writing, review and editing, supervision.

## Declaration of competing interest

The authors declare that they have no known competing financial interests or personal relationships that could have appeared to influence the work reported in this paper.

## Acknowledgment

The authors would like to acknowledge Léon Rohrbach from the University of Groningen for help with the GC-TCD and GC × GC-FID analyses; H.H. van de Bovenkamp, Fenna Heins, and Monique Bernardes Figueirêdo from the University of Groningen, for technical and practical assistance. The Multidisciplinary Research Platform “Ghent Bio-economy” is acknowledged for providing access to the lignin feedstock. The LOTUS Programme of the European Union is acknowledged for providing a doctoral scholarship to Neil Priharto.

## Appendix A. Supplementary data

Supplementary data to this article can be found online at https://doi.org/10.1016/j.fuproc.2020.106466.

## References

[1] X. Miao, Q. Wu, High yield bio-oil production from fast pyrolysis by metabolic controlling of Chlorella protothecoides, J. Biotechnol. 110 (2004) 85–93, https://doi.org/10.1016/j.jbiotec.2004.01.013.
[2] S.W. Kim, B.S. Koo, D.H. Lee, A comparative study of bio-oils from pyrolysis of microalgae and oil seed waste in a fluidized bed, Bioresour. Technol. 162 (2014) 96–102, https://doi.org/10.1016/j.biortech.2014.03.136.
[3] W. Peng, Q. Wu, P. Tu, N. Zhao, Pyrolytic characteristics of microalgae as renewable energy source determined by thermogravimetric analysis, Bioresour. Technol. 80 (1999) 367–371, https://doi.org/10.1109/ICON.1999.796199.
[4] P. Biller, B.K. Sharma, B. Kunwar, A.B. Ross, Hydroprocessing of bio-crude from continuous hydrothermal liquefaction of microalgae, Fuel. 159 (2015) 197–205, https://doi.org/10.1016/j.fuel.2015.06.077.
[5] Z. Du, M. Mohr, X. Ma, Y. Cheng, X. Lin, Y. Liu, W. Zhou, P. Chen, R. Ruan, Hydrothermal pretreatment of microalgae for production of pyrolytic bio-oil with a low nitrogen content, Bioresour. Technol. 120 (2012) 13–18, https://doi.org/10.1016/j.biortech.2012.06.007.
[6] K. Azizi, M. Keshavarz Moraveji, H. Abedini Najafabadi, A review on bio-fuel production from microalgal biomass by using pyrolysis method, Renew. Sust. Energ. Rev. 82 (2018) 3046–3059, https://doi.org/10.1016/j.rser.2017.10.033.
[7] C.Y. Chen, X.Q. Zhao, H.W. Yen, S.H. Ho, C.L. Cheng, D.J. Lee, F.W. Bai, J.S. Chang, Microalgae-based carbohydrates for biofuel production, Biochem. Eng. J. 78 (2013) 1–10, https://doi.org/10.1016/j.bej.2013.03.006.
[8] A. Campanella, R. Muncrief, M.P. Harold, D.C. Griffith, N.M. Whitton, R.S. Weber, Thermolysis of microalgae and duckweed in a CO 2-swept fixed-bed reactor: bio-oil yield and compositional effects, Bioresour. Technol. 109 (2012) 154–162, https://doi.org/10.1016/j.biortech.2011.12.115.
[9] M. Adamczyk, M. Sajdak, Pyrolysis behaviours of microalgae Nannochloropsis gaditana, Waste and Biomass Valorization. 9 (2018) 2221–2235, https://doi.org/10.1007/s12649-017-9996-8.
[10] K. Wang, R.C. Brown, S. Homsy, L. Martinez, S.S. Sidhu, Fast pyrolysis of microalgae remnants in a fluidized bed reactor for bio-oil and biochar production, Bioresour. Technol. 127 (2013) 494–499, https://doi.org/10.1016/j.biortech.2012.08.016.
[11] K. Kebelmann, A. Hornung, U. Karsten, G. Griffiths, Intermediate pyrolysis and product identification by TGA and Py-GC/MS of green microalgae and their extracted protein and lipid components, Biomass Bioenergy 49 (2013) 38–48, https://doi.org/10.1016/j.biombioe.2012.12.006.
[12] X. Miao, Q. Wu, C. Yang, Fast pyrolysis of microalgae to produce renewable fuels, J. Anal. Appl. Pyrolysis 71 (2004) 855–863, https://doi.org/10.1016/j.jaap.2003.11.004.
[13] A. Demirbaş, Mechanisms of liquefaction and pyrolysis reactions of biomass, Energy Convers. Manag. 41 (2000) 633–646, https://doi.org/10.1016/S0196-8904(99)00130-2.
[14] D. López-González, M. Fernandez-Lopez, J.L. Valverde, L. Sanchez-Silva, Pyrolysis of three different types of microalgae: kinetic and evolved gas analysis, Energy. 73 (2014) 33–43, https://doi.org/10.1016/j.energy.2014.05.008.
[15] X. Gong, B. Zhang, Y. Zhang, Y. Huang, M. Xu, Investigation on pyrolysis of low lipid microalgae Chlorella vulgaris and Dunaliella salina, Energy and Fuels. 28 (2014) 95–103, https://doi.org/10.1021/ef401500z.
[16] F. Sotoudehniakarani, A. Alayat, A.G. McDonald, Characterization and comparison of pyrolysis products from fast pyrolysis of commercial Chlorella vulgaris and cultivated microalgae, J. Anal. Appl. Pyrolysis (2019), https://doi.org/10.1016/j.jaap.2019.02.014.
[17] L.O. Garciano, N.H. Tran, G.S.K. Kannangara, A.S. Milev, M.A. Wilson, D.M. McKirdy, P.A. Hall, Pyrolysis of a naturally dried botryococcus braunii residue, Energy and Fuels. 26 (2012) 3874–3881, https://doi.org/10.1021/ef300451s.
[18] M. Francavilla, P. Kamaterou, S. Intini, M. Monteleone, A. Zabaniotou, Cascading microalgae biorefinery: fast pyrolysis of Dunaliella tertiolecta lipid extracted-residue, Algal Res. 11 (2015) 184–193, https://doi.org/10.1016/j.algal.2015.06.017.
[19] X. Wang, L. Sheng, X. Yang, Pyrolysis characteristics and pathways of protein, lipid and carbohydrate isolated from microalgae Nannochloropsis sp, Bioresour. Technol. 229 (2017) 119–125, https://doi.org/10.1016/j.biortech.2017.01.018.
[20] A. Gutierrez, R.K. Kaila, M.L. Honkela, R. Slioor, A.O.I. Krause, Hydrodeoxygenation of guaiacol on noble metal catalysts, Catal. Today 147 (2009) 239–246, https://doi.org/10.1016/j.cattod.2008.10.037.
[21] M.S. Haider, D. Castello, K.M. Michalski, T.H. Pedersen, L.A. Rosendahl, Catalytic hydrotreatment of microalgae biocrude from continuous hydrothermal liquefaction: heteroatom removal and their distribution in distillation cuts, Energies 11 (2018), https://doi.org/10.3390/en11123360.
[22] A.R. Ardiyanti, A. Gutierrez, M.L. Honkela, A.O.I. Krause, H.J. Heeres, Hydrotreatment of wood-based pyrolysis oil using zirconia-supported mono- and bimetallic (Pt, Pd, Rh) catalysts, Appl. Catal. A Gen. 407 (2011) 56–66, https://doi.org/10.1016/j.apcata.2011.08.024.
[23] X. Zhang, T. Wang, L. Ma, Q. Zhang, T. Jiang, Hydrotreatment of bio-oil over Ni-based catalyst, Bioresour. Technol. 127 (2013) 306–311, https://doi.org/10.1016/j.biortech.2012.07.119.
[24] A. Ardiyanti, Hydrotreatment of Fast Pyrolysis Oil: Catalyst Development and Process-Product Relations, (2013) (Groningen: s.n.).
[25] A. Kloekhorst, J. Wildschut, H.J. Heeres, Catalytic hydrotreatment of pyrolytic lignins to give alkylphenolics and aromatics using a supported Ru catalyst, Catal. Sci. Technol. 4 (2014) 2367–2377, https://doi.org/10.1039/C4CY00242C.
[26] J. Wildschut, F.H. Mahfud, R.H. Venderbosch, H.J. Heeres, Hydrotreatment of fast pyrolysis oil using heterogeneous noble-metal catalysts, Ind. Eng. Chem. Res. 48 (2009) 10324–10334, https://doi.org/10.1021/ie9006003.
[27] A. Oasmaa, E. Kuoppala, A. Ardiyanti, R.H. Venderbosch, H.J. Heeres, Characterization of hydrotreated fast pyrolysis liquids, Energy and Fuels. 24 (2010) 5264–5272, https://doi.org/10.1021/ef100573q.
[28] R.H. Venderbosch, A.R. Ardiyanti, J. Wildschut, A. Oasmaa, H.J. Heeres, Stabilization of biomass-derived pyrolysis oils, J. Chem. Technol. Biotechnol. 85 (2010) 674–686, https://doi.org/10.1002/jctb.2354.
[29] D.C. Elliott, Biofuel from fast pyrolysis and catalytic hydrodeoxygenation, Curr. Opin. Chem. Eng. 9 (2015) 59–65, https://doi.org/10.1016/j.coche.2015.08.008.
[30] Q. Guo, M. Wu, K. Wang, L. Zhang, X. Xu, Catalytic hydrodeoxygenation of algae bio-oil over bimetallic Ni-Cu/ZrO2 catalysts, Ind. Eng. Chem. Res. 54 (2015) 890–899, https://doi.org/10.1021/ie5042935.
[31] W. Zhong, Q. Guo, X. Wang, L. Zhang, Catalytic hydroprocessing of fast pyrolysis bio-oil from Chlorella, J. Fuel Chem. Technol. 41 (2013) 571–578, https://doi.org/10.1016/s1872-5813(13)60030-4.
[32] W. Yin, R.H. Venderbosch, G. Bottari, K.K. Krawzcyk, K. Barta, H.J. Heeres, Catalytic upgrading of sugar fractions from pyrolysis oils in supercritical monoalcohols over Cu doped porous metal oxide, Appl. Catal. B Environ. 166–167 (2015) 56–65, https://doi.org/10.1016/j.apcatb.2014.10.065.
[33] A. Kloekhorst, H.J. Heeres, Catalytic hydrotreatment of alcell lignin using supported Ru, Pd, and Cu catalysts, ACS Sustain. Chem. Eng. 3 (2015) 1905–1914,

https://doi.org/10.1021/acssuschemeng.5b00041.
[34] C.A.L. Cardoso, M.E. Machado, F.S. Maia, G.J. Arruda, E.B. Caramão, GCxGC-TOF/MS analysis of bio-oils obtained from pyrolysis of acuri and baru residues, J. Braz. Chem. Soc. 27 (2016) 2149–2159, https://doi.org/10.5935/0103-5053.20160081.
[35] J.H. Marsman, J. Wildschut, F. Mahfud, H.J. Heeres, Identification of components in fast pyrolysis oil and upgraded products by comprehensive two-dimensional gas chromatography and flame ionisation detection, J. Chromatogr. A 1150 (2007) 21–27, https://doi.org/10.1016/j.chroma.2006.11.047.
[36] I.D.V. Torri, V. Paasikallio, C.S. Faccini, R. Huff, E.B. Caramão, V. Sacon, A. Oasmaa, C.A. Zini, Bio-oil production of softwood and hardwood forest industry residues through fast and intermediate pyrolysis and its chromatographic characterization, Bioresour. Technol. 200 (2016) 680–690, https://doi.org/10.1016/j.biortech.2015.10.086.
[37] N. Priharto, F. Ronsse, W. Prins, I. Hita, P.J. Deuss, H.J. Heeres, Hydrotreatment of pyrolysis liquids derived from second-generation bioethanol production residues over NiMo and CoMo catalysts, Biomass Bioenergy 126 (2019) 84–93, https://doi.org/10.1016/j.biombioe.2019.05.005.
[38] C.S. Lancefield, I. Panovic, P.J. Deuss, K. Barta, N.J. Westwood, Pre-treatment of lignocellulosic feedstocks using biorenewable alcohols: towards complete biomass valorisation, Green Chem. 19 (2017) 202–214, https://doi.org/10.1039/C6GC02739C.
[39] D. López Barreiro, S. Riede, U. Hornung, A. Kruse, W. Prins, Hydrothermal liquefaction of microalgae: effect on the product yields of the addition of an organic solvent to separate the aqueous phase and the biocrude oil, Algal Res. 12 (2015) 206–212, https://doi.org/10.1016/j.algal.2015.08.025.
[40] D.L. Barreiro, B.R. Gómez, U. Hornung, A. Kruse, W. Prins, Hydrothermal liquefaction of microalgae in a continuous stirred-tank reactor, Energy and Fuels. 29 (2015) 6422–6432, https://doi.org/10.1021/acs.energyfuels.5b02099.
[41] T. Mathimani, A. Baldinelli, K. Rajendran, D. Prabakar, M. Matheswaran, R. Pieter van Leeuwen, A. Pugazhendhi, Review on cultivation and thermochemical conversion of microalgae to fuels and chemicals: process evaluation and knowledge gaps, J. Clean. Prod. 208 (2019) 1053–1064, https://doi.org/10.1016/j.jclepro.2018.10.096.
[42] V. Anand, R. Gautam, R. Vinu, Non-catalytic and catalytic fast pyrolysis of Schizochytrium limacinum microalga, Fuel. 205 (2017) 1–10, https://doi.org/10.1016/j.fuel.2017.05.049.
[43] G. Li, Y. Zhou, F. Ji, Y. Liu, B. Adhikari, L. Tian, Z. Ma, R. Dong, Yield and characteristics of pyrolysis products obtained from Schizochytrium limacinum under different temperature regimes, Energies. 6 (2013) 3339–3352, https://doi.org/10.3390/en6073339.
[44] M.A. Borowitzka, Algae Oils for Biofuels: Chemistry, Physiology, and Production, second ed., AOCS Press, 2010, https://doi.org/10.1016/B978-1-893997-73-8.50017-7 ©2010. All rights reserved..
[45] R.R. Narala, S. Garg, K.K. Sharma, S.R. Thomas-Hall, M. Deme, Y. Li, P.M. Schenk, Comparison of microalgae cultivation in photobioreactor, open raceway pond, and a two-stage hybrid system, Front. Energy Res. 4 (2016), https://doi.org/10.3389/fenrg.2016.00029.
[46] M.M. Pacheco, M. Hoeltz, M.S.A. Moraes, R.C.S. Schneider, Microalgae: cultivation techniques and wastewater phycoremediation, J. Environ. Sci. Heal. - Part A Toxic/Hazardous Subst. Environ. Eng. 50 (2015) 585–601, https://doi.org/10.1080/10934529.2015.994951.
[47] R. Kothari, A. Pandey, S. Ahmad, A. Kumar, V.V. Pathak, V.V. Tyagi, Microalgal cultivation for value-added products: a critical enviro-economical assessment, 3 Biotech. 7 (2017) 1–15, https://doi.org/10.1007/s13205-017-0812-8.
[48] S.T. Jacobs, Bentayan Field: unique method of heavy oil production, South Sumatra, Proc. Indon Pet. Assoc., 15th Ann. Conv. Indonesian Petroleum Association (IPA), Jakarta, 1986, , https://doi.org/10.29118/IPA.2547.65.77.
[49] X. Qing, M. Xiaoqian, Y. Zhaosheng, C. Zilin, L. Changming, Decomposition characteristics and kinetics of microalgae in N2 and CO2 atmospheres by a thermogravimetry, J. Combust. 2017 (2017), https://doi.org/10.1155/2017/6160234.
[50] J.A. Maga, Thermal Decomposition of Carbohydrates, (1989), pp. 32–39, https://doi.org/10.1021/bk-1989-0409.ch004.
[51] H. Sugisawa, The Thermal Degradation Of Sugars. II. The volatile decomposition products of glucose caramel, J. Food Sci. 31 (1966) 381–385.
[52] L. Sanchez-Silva, D. López-González, A.M. Garcia-Minguillan, J.L. Valverde, Pyrolysis, combustion and gasification characteristics of Nannochloropsis gaditana microalgae, Bioresour. Technol. 130 (2013) 321–331, https://doi.org/10.1016/j.biortech.2012.12.002.
[53] P. Duan, P.E. Savage, Upgrading of crude algal bio-oil in supercritical water, Bioresour. Technol. 102 (2011) 1899–1906, https://doi.org/10.1016/j.biortech.2010.08.013.
[54] L. Zhou, A. Lawal, Evaluation of presulfided NiMo/γ-Al2O3 for hydrodeoxygenation of microalgae oil to produce green diesel, Energy and Fuels. 29 (2015) 262–272, https://doi.org/10.1021/ef502258q.
[55] A.V. Bridgwater, Review of fast pyrolysis of biomass and product upgrading, Biomass Bioenergy 38 (2012) 68–94, https://doi.org/10.1016/j.biombioe.2011.01.048.
[56] H. Yao, G. Wang, C. Zuo, C. Li, E. Wang, S. Zhang, Deep hydrodenitrification of pyridine by solid catalyst coupling with ionic liquids under mild conditions, Green Chem. 19 (2017) 1692–1700, https://doi.org/10.1039/c6gc03432b.
[57] B. Donnis, R.G. Egeberg, P. Blom, K.G. Knudsen, Hydroprocessing of bio-oils and oxygenates to hydrocarbons. Understanding the reaction routes, Top. Catal. 52 (2009) 229–240, https://doi.org/10.1007/s11244-008-9159-z.
[58] N. Hao, H. Ben, C.G. Yoo, S. Adhikari, A.J. Ragauskas, Review of NMR characterization of pyrolysis oils, Energy and Fuels. 30 (2016) 6863–6880, https://doi.org/10.1021/acs.energyfuels.6b01002.
[59] Y. Yu, Y.W. Chua, H. Wu, Characterization of pyrolytic sugars in bio-oil produced from biomass fast pyrolysis, Energy and Fuels. 30 (2016) 4145–4149, https://doi.org/10.1021/acs.energyfuels.6b00464.
[60] J.G. Speight, The chemistry and technology of petroleum, Fuel Process. Technol. 5 (1982) 325–326, https://doi.org/10.1016/0378-3820(82)90026-1.
[61] A.J.J. Straathof, A. Bampouli, Potential of commodity chemicals to become bio-based according to maximum yields and petrochemical prices, Biofuels Bioprod. Bioref. 11 (2017) 798–810, https://doi.org/10.1002/bbb1786.
[62] https://www.ceicdata.com/en/china/china-petroleum–chemical-industry-association-petrochemical-price-organic-chemical-material/cn-market-price-monthly-avg-organic-chemical-material-pyridine-999.